Functional-Group Compatible Electrooxidation Synthesis of Key Antibiotic Intermediate Rifamycin O

Lihao Liu,[+[a]] Shaoming Zhu,[+[c]] Kai Li,[+[a]] Yuhang Wang,[a] Suiqin Li,[d] Jiahui He,[a] Pan Hu,[a] Chuang Qi,[a] Ruixiang Liang,[a] Xing Zhong,[*[a] [b]] Jianguo Wang [a]

[a] State Key Laboratory of Green Chemical Synthesis and Conversion, Zhejiang Key Laboratory of Surface and Interface Science and Engineering for Catalysts, College of Chemical Engineering, Zhejiang University of Technology, Hangzhou 310032, China

[b] Innovation Research Center for Advanced Environmental Technology, Eco-Industrial Innovation Institute, ZJUT, Rong-Chang East Road, Quzhou 324400, China

[c] Zhejiang Changhai Pharmaceuticals Co., Ltd., Shaoxing 312000, China

[d] Zhejiang Key Laboratory of Functional ionic membrane Materials and Technology for Hydrogen Production, Shaoxing University, Shaoxing 312000, China

[#]L. Liu, S. Zhu, K. Li contribute to this work equally.

*Correspondence and requests for materials should be addressed to X. Zhong (email: zhongx@zjut.edu.cn).

.

1. Experimental procedures

1.1. Divided batch electrolyzer reaction

The electrooxidation of RB were performed using an Ivium-n-Stat workstation in a two-electrode system (Fig. S1). Using AEM8040 as the membrane. The anolyte was composed of RB (0.36 g, 0.48 mmol), 0.05 mol/L $LiClO_4$, 0.5 mL H_2O in 25 mL MeOH solution, with constant current of 20 mA (current density is 5 mA/cm^2) was carried out. The catholyte was composed of 3 M NaOH. The working electrode was composed of GF (4 cm^2, thickness 3 mm), the counter electrode consisted of Pt plate (4 cm^2). The reaction was terminated when the electric quantity reaches 1.8 F/mol. A magnetic stir bar (2 cm) was used, and the reaction mixture was stirred (400 rpm) during electrolysis. The yield of product was determined by HPLC and measured by external standard method (Fig. S2).

1.2. Divided flow electrolyzer reaction

The electrooxidation of RB were performed using an Ivium-n-Stat workstation in a two-electrode system (Fig. S1). Using AEM8040 as the membrane. The anolyte was composed of RB (1.44 g, 1.92 mmol), 0.05 mol/L $LiClO_4$, 2 mL H_2O in 100 mL MeOH solution, with constant current of 100 mA (current density is 10 mA/cm^2) was carried out. The catholyte was composed of 3 M NaOH. The working electrode was composed of GF (10 cm^2, thickness 6 mm), the counter electrode consisted of Nickl form (10 cm^2). The reaction was terminated when the electric quantity reaches 1.8 F/mol. The cell voltage during constant current electrolysis was monitored. The magneton was stirred to ensure uniform mixing of the reaction solution, and a peristaltic pump was employed

to pump electrolytes into the reaction system. A flow rates of 338 mL/min was selected as optimal for the experiments. At the end of the reaction, the reaction solution was concentrated under reduced pressure on a rotary evaporator until a small amount of solid was produced. The solution was then cooled and recrystallized in order to obtain the product, rifamycin O. The yield of product was determined by HPLC and measured by external standard method (Fig. S2).

The stage electrolysis study utilizes the same methodological approach as previously delineated, with the exception that, upon the application of the current, the initial electric quantity of 1.62 F/mol was conducted at 40 mA/cm^2, and the final quantity of 0.18 F/mol was conducted at 10 mA/cm^2.

1.3. Scale-up amplification experiment

The electrooxidation of RB were performed using an Ivium-n-Stat workstation in a two-electrode system (Fig. S1). Using AEM8040 as the membrane. The anolyte was composed of RB (50 g), 0.05 mol/L KCl, 80 mL H_2O in 4 L MeOH solution. The initial electric quantity of 1.62 F/mol was conducted at 16A (40 mA/cm^2), and the final quantity of 0.25 F/mol was conducted at 4A (10 mA/cm^2).

The catholyte was composed of 3 M NaOH. The working electrode was composed of GF (400 cm^2, thickness 15 mm), the counter electrode consisted of Nickl form (400 cm^2). The cell voltage during constant current electrolysis was monitored. The magneton was stirred to ensure uniform mixing of the reaction solution, and a diaphragm pump was employed to pump electrolytes into the reaction system. A flow rates of 338 mL/min was selected as optimal for the experiments. At the end of the

reaction, the reaction solution was concentrated under reduced pressure on a rotary evaporator until a small amount of solid was produced. The solution was then cooled and recrystallized in order to obtain the product, rifamycin O. The yield of product was determined by HPLC and measured by external standard method (Fig. S2).

1.4. In situ electrochemical IRAS measurement.

In situ infrared reflection absorption spectroscopy (IRAS) measurements were performed on ThermoFisher Nicolet iS50 (dector: MCT/A; number of scans:32; moving mirror speed: 1.8988). A custom three-chamber electrochemical cell was used and filled with 20 mL MeOH solution containing a predetermined amount of $LiClO_4$, H_2O and RB. The anode and reference electrodes were a platinum sheet and an SCE electrode, respectively. The 10 mg graphite was dissolved in 990 μL ethanol and 10 μL Nafion, and 1 mL was dropped on the surface of the gold film, and thoroughly dried under an infrared lamp. Before sample measurements, a background spectrum of reaction solution was recorded and ratioed against each spectrum of the aqueous sample. Between each measurement, the sample cell was thoroughly washed with MeOH and water, followed by drying.

1.5. Calculation of conversion, selectivity, faradaic efficiency and space-time yield

The conversion (%) and the selectivity (%) were calculated using equations (1) and (2):

$$Conversion\ (\%) = \frac{mol\ of\ substrate\ consumed}{mol\ of\ initial\ substrate} \times 100\%\ , \qquad (1)$$

$$Selectivity\ (\%) = \frac{mol\ of\ main\ product\ formed}{mol\ of\ substrate\ consumed} \times 100\%\,, \quad (2)$$

The Faradaic efficiency (FE) formation was calculated using equations (3):

$$FE\ (\%) = \frac{mol\ of\ main\ product\ \ formed}{total\ charge\ passed\ /\ (n\ \times F)} \times 100\%\,, \quad (3)$$

Here, n represents number of electron transfers, F represents the Faraday constant (96485 C mol^{-1}).

The space-time yield (Y_{ST}, kg/(m^3·h)) was calculated as shown in (4):

$$Y_{ST}\left(kg/\left(m^3 \cdot h\right)\right) = \frac{m}{t \times V_R}, \quad (4)$$

Here, m is the quality of products (kg), t is the reaction time (h), V_R is the volume of reactor (m^3).

1.6. Calculation of energy consumption in scale-up amplification experiment

The energy consumption was calculated using the following formula：

$$E(kWh/kg) = \frac{Z \times F \times V}{\eta \times M \times 3600}$$

where:

Z = 2 (number of electrons transferred)

F = 96485 C/mol (Faraday constant)

V = 3V (average cell voltage, obtained from Fig. 5)

η = 79% (Faradaic efficiency)

M = 753.79 g/mol (molecular weight of product)

The factor 3600 converts J/g to kWh/kg ($1\ \text{kWh} = 3.6 \times 10^6$ J).

Based on these values, the calculated energy consumption is $E = 0.27$ kWh/kg.

2. Supplementary Results

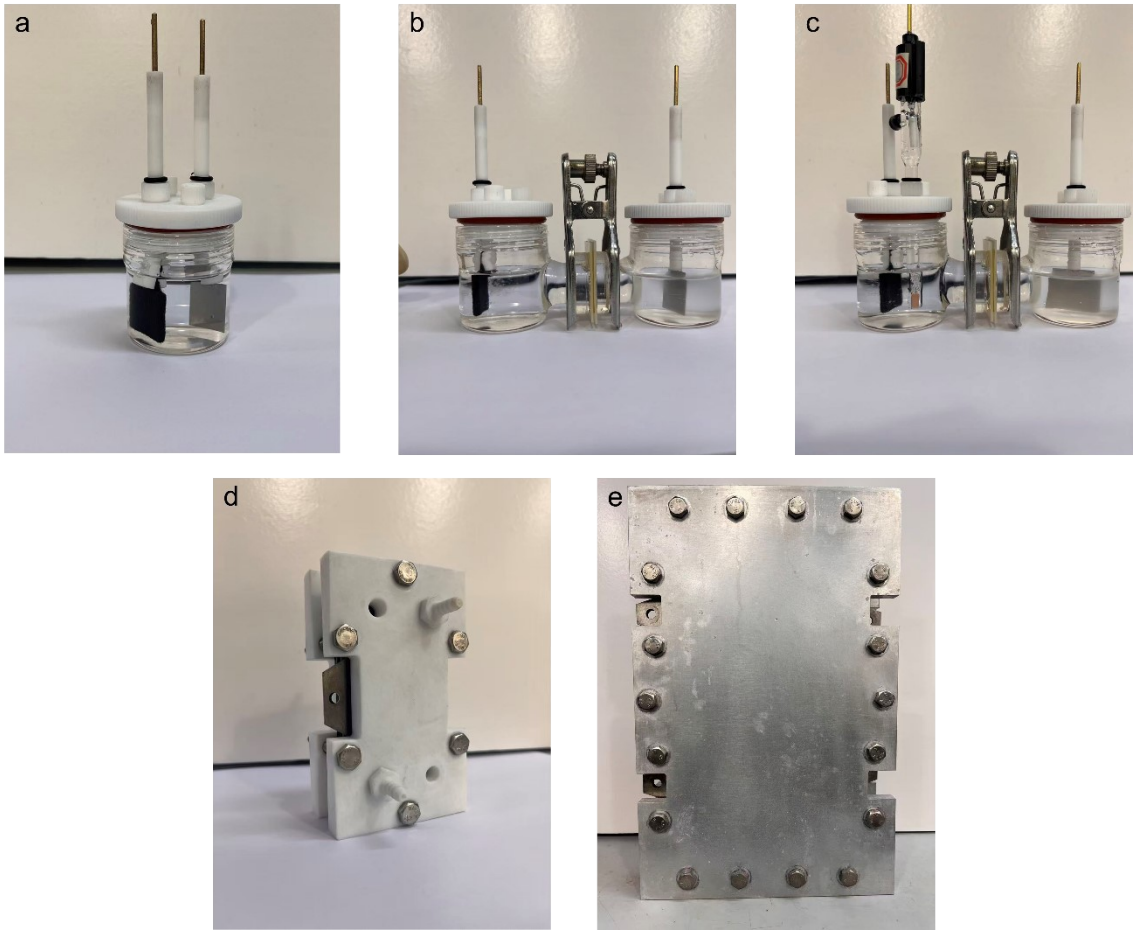

Fig. S1 The photograph of different electrolyzers.

(a) Two electrode batch electrolyzer: applied to undivided batch electrolyzer reaction.

(b) Two electrode H-type electrolyzer: applied to divided batch electrolyzer reaction.

(c) Three electrode H-type electrolyzer: applied to electrochemical measurements and constant potential electrolysis.

(d) Small-scale flow electrolyzer: applied to divided flow electrolyzer reaction.

(e) Large-scale electrolyzer: applied to scale-up amplification experiment.

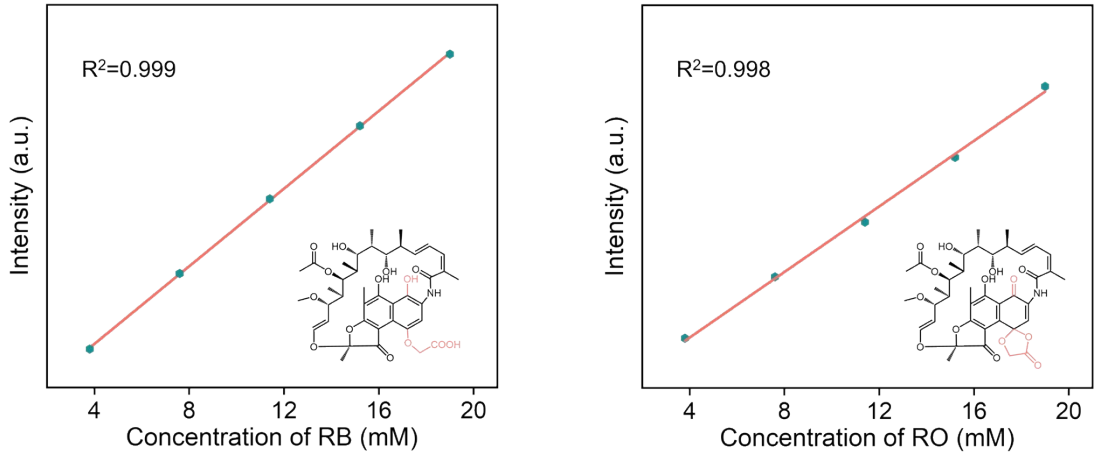

Fig. S2 HPLC external standard curves of rifamycin B and rifamycin O.

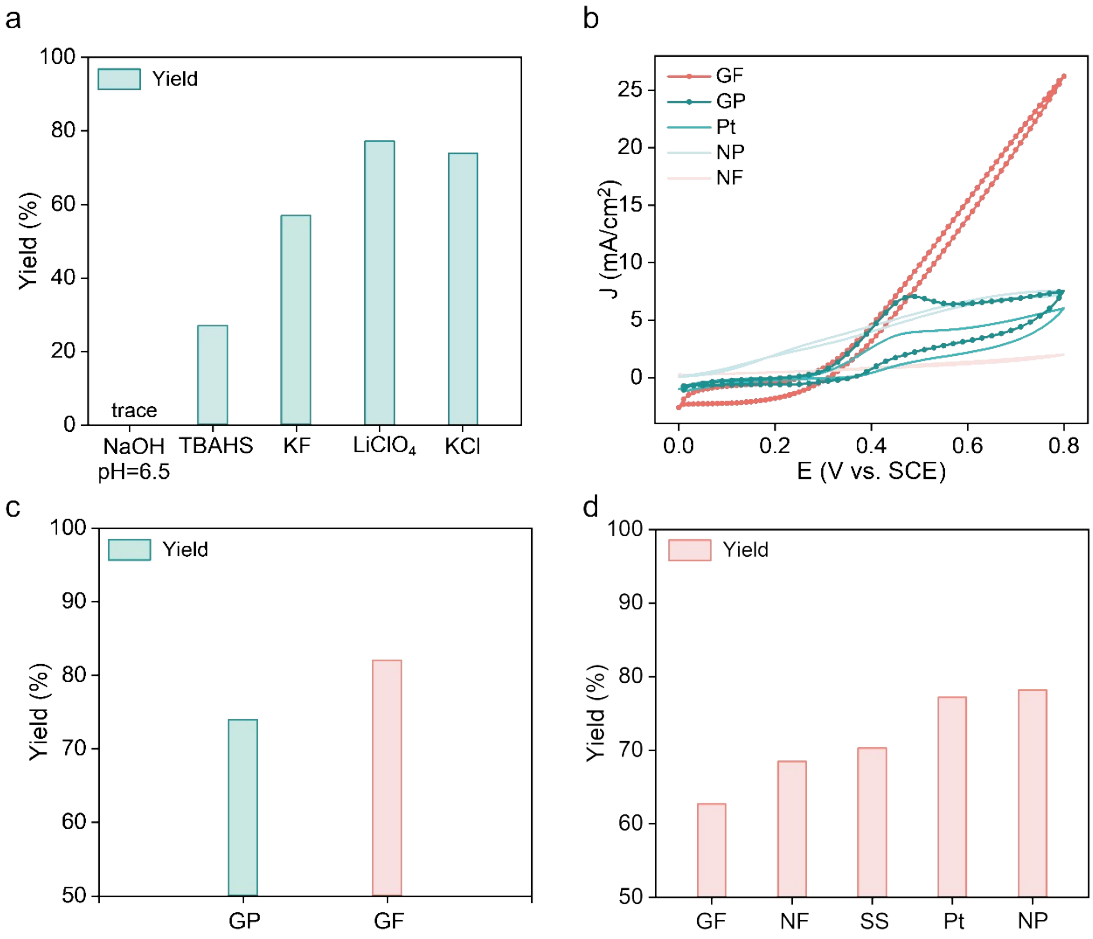

Fig. S3 (a)RO yield in different electrolytes. (b) CV analysis of different anode electrode. (c) RO yield for GP or GF as anode electrode. (d) RO yield in different cathode electrode.

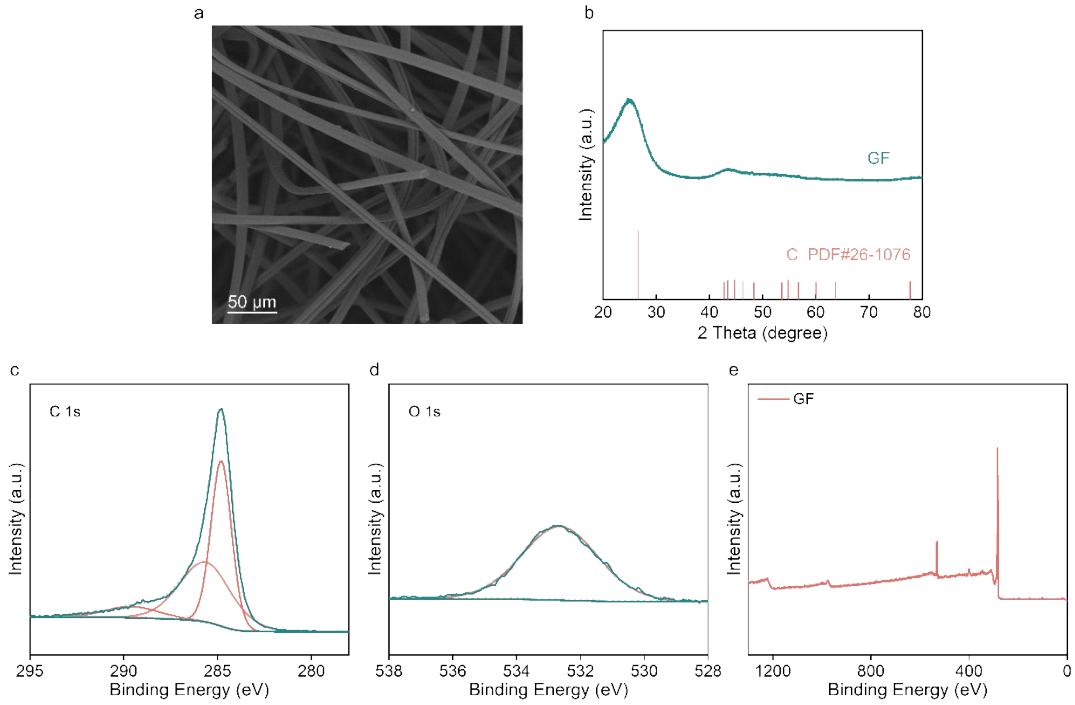

Fig. S4 (a) SEM image and (b) XRD spectra of Graphite felt. XPS spectra of (c) C 1s and (d) O 1s and (e) survey XPS spectra of Graphite felt

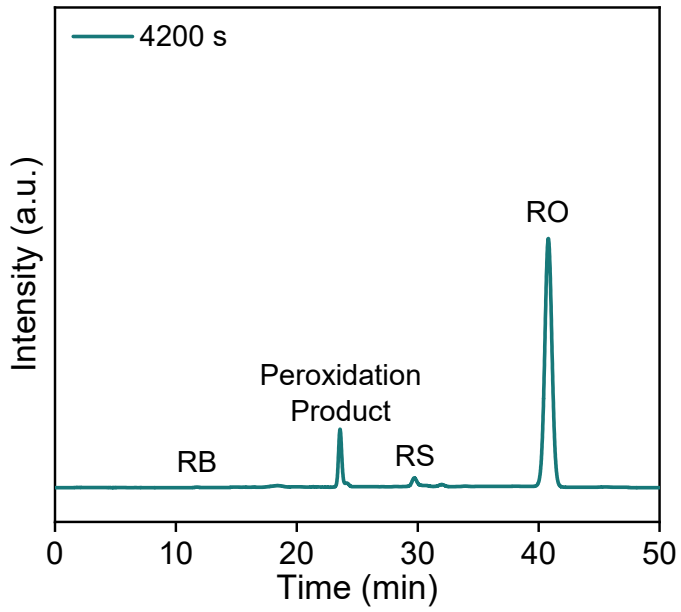

Fig. S5 HPLC chromatogram at the end of the electrooxidation of RB.

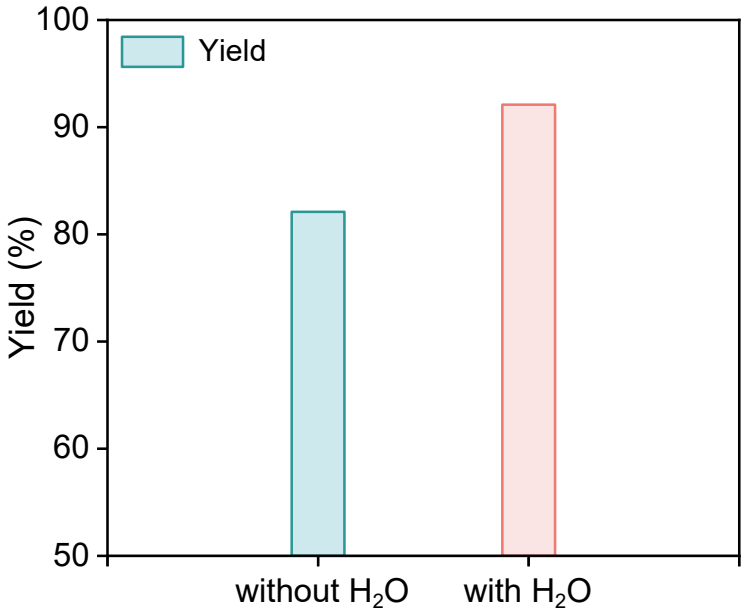

Fig. S6 Yield comparison of the electrooxidation of RB (KCl as electrolyte).

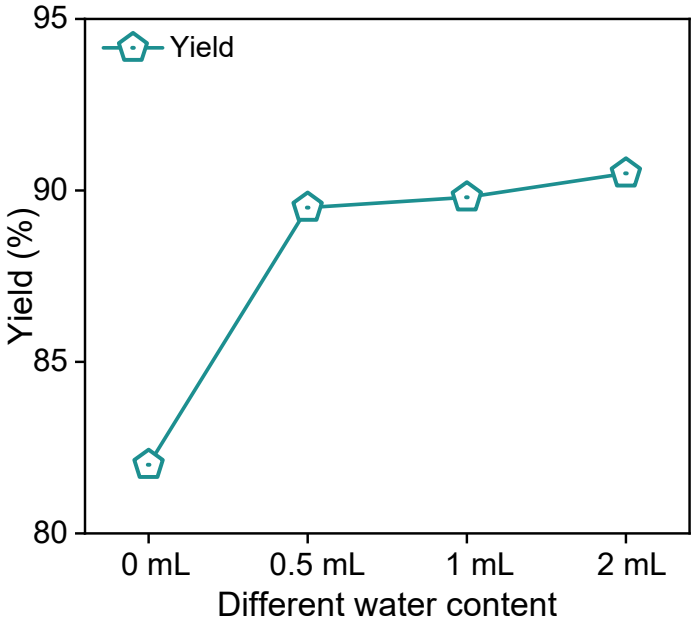

Fig. S7 Effect of different water quantity on the electrooxidation of RB ($LiClO_4$ as electrolyte).

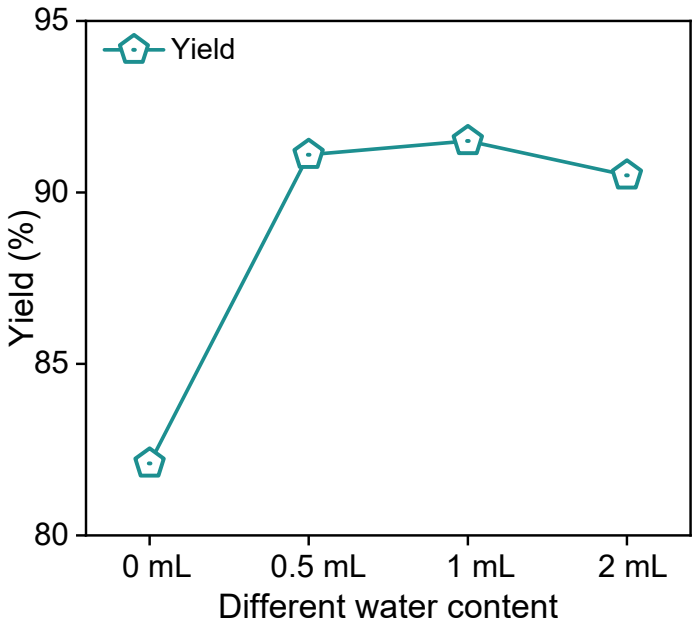

Fig. S8 Effect of different water quantity on the electrooxidation of RB (KCl as electrolyte).

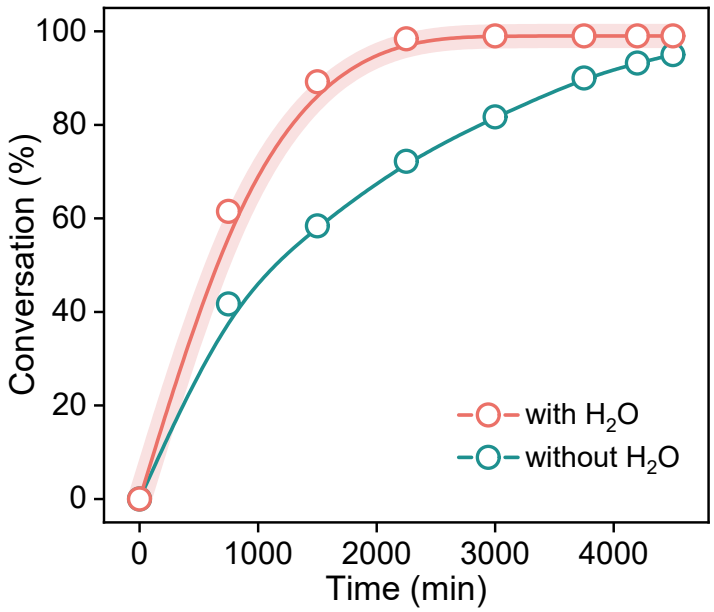

Fig. S9 Conversion in the presence or absence of water.

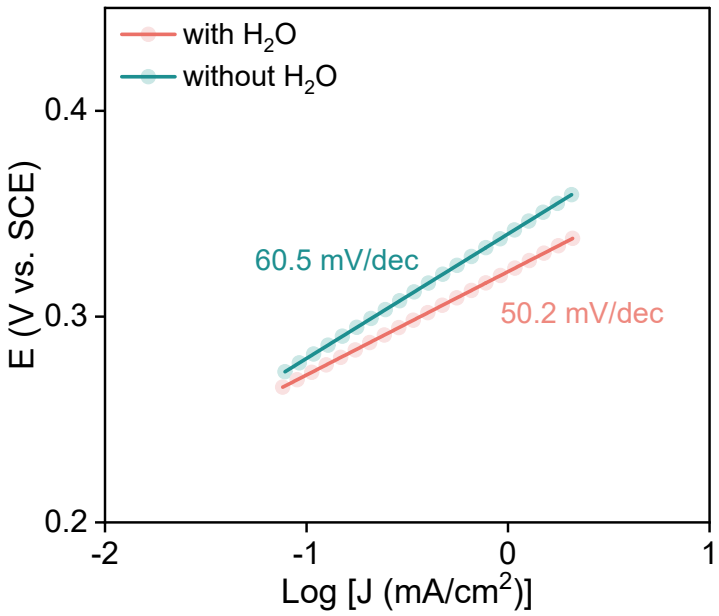

Fig. S10 Tafel plot for the electrooxidation of RB in the presence or absence of water.

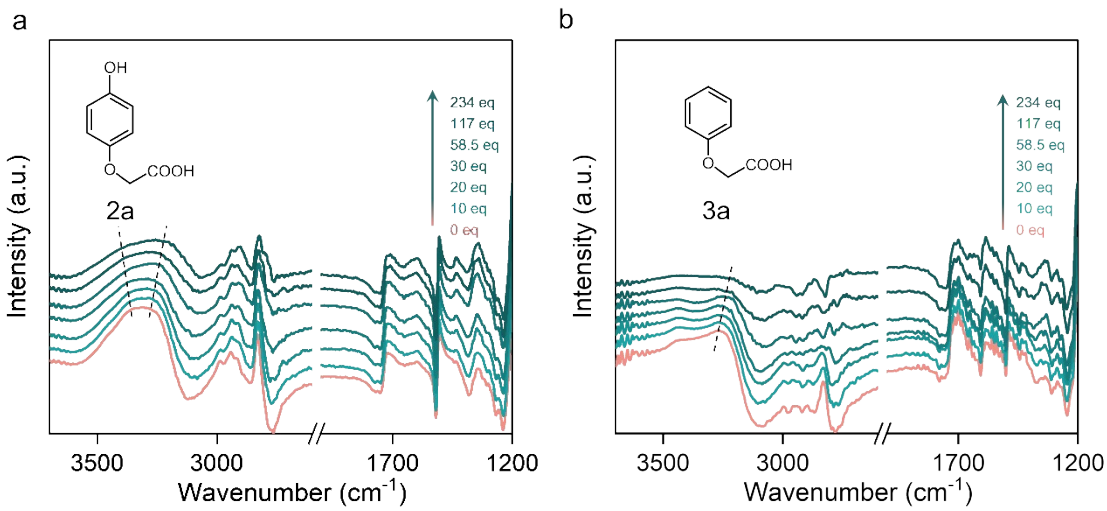

Fig. S11 FTIR spectra of 2a (a) and 3a (b) in methanol solutions with different water contents.

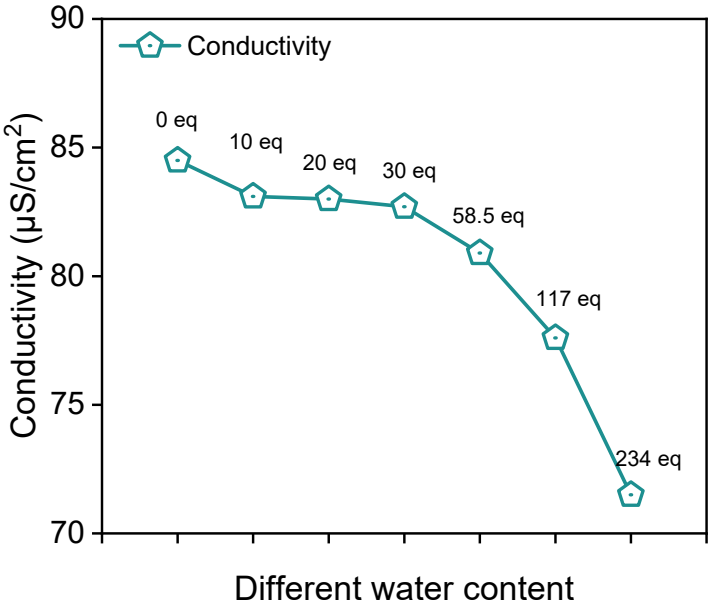

Fig. S12 Conductivity in different water ($LiClO_4$ as electrolyte).

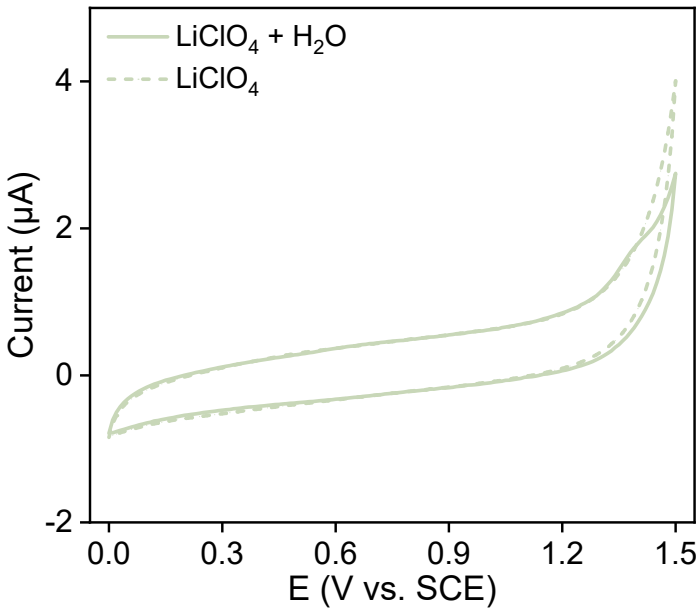

Fig. S13 CV analysis in the presence or absence of water.

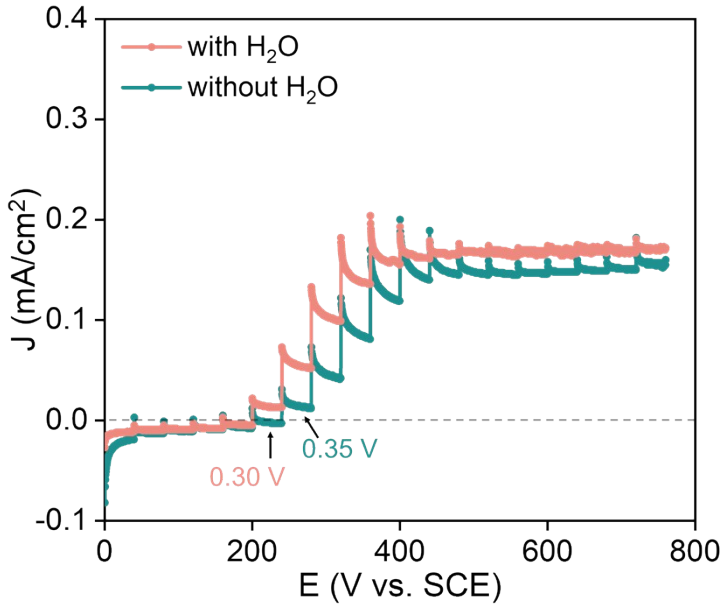

Fig. S14 i-E plot of electrooxidation of RB under in-situ IRAS testing conditions.

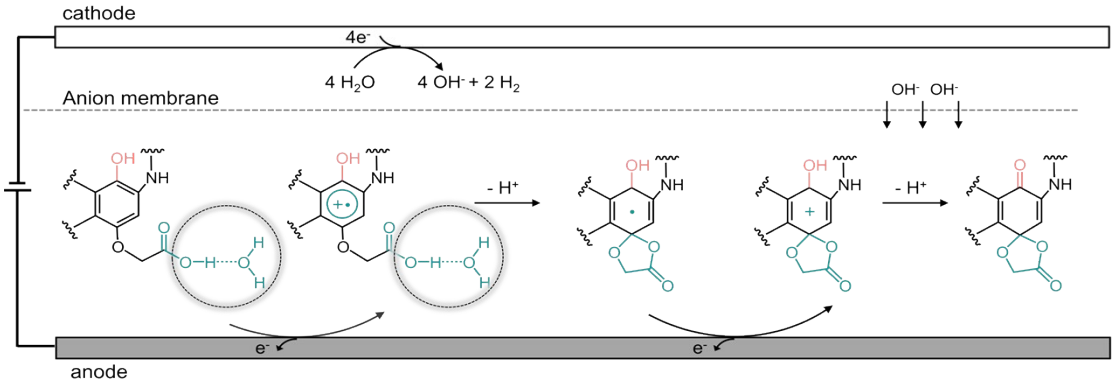

Fig. S15 Possible electrooxidation mechanism of RB

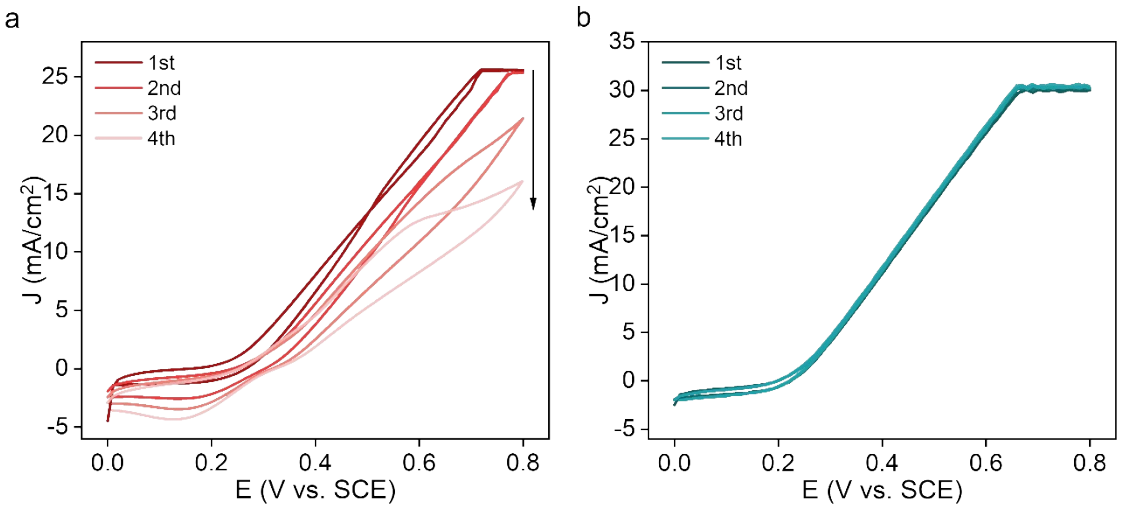

Fig. S16 CV analysis for the electrooxidation of RB in the absence (a) or presence (b) of stir.

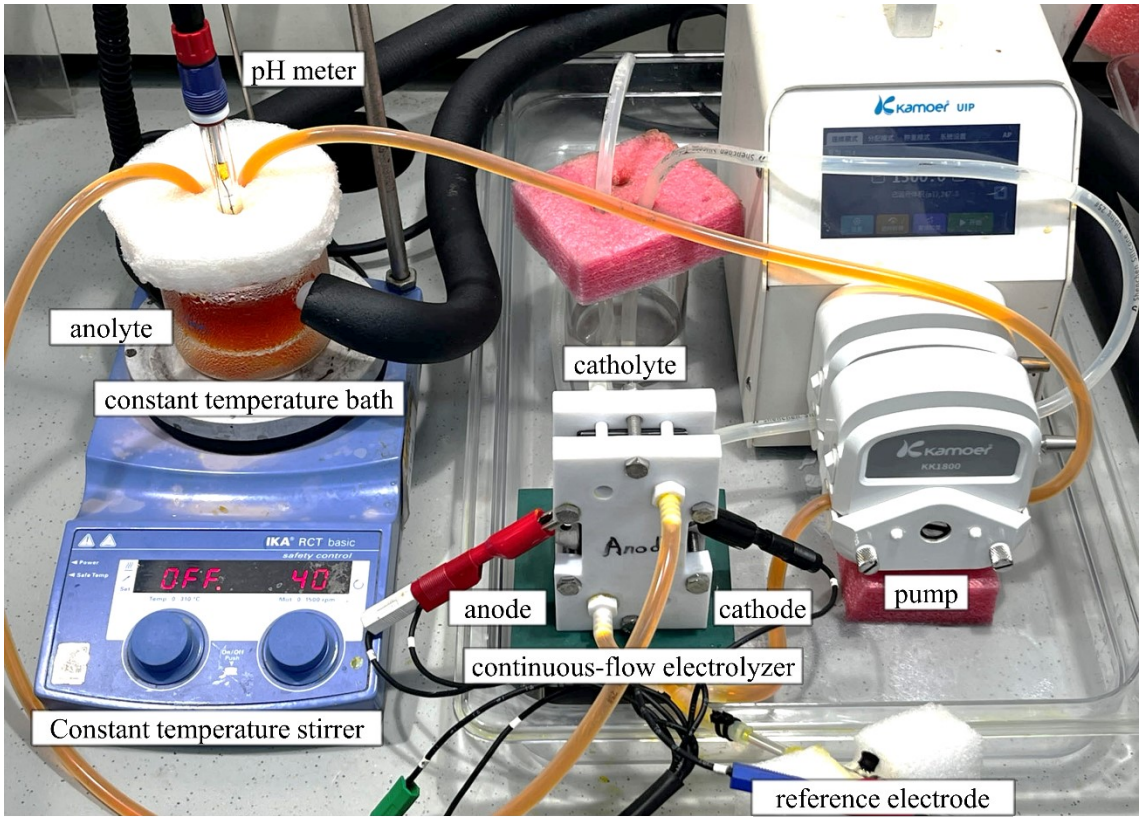

Fig. S17 Electrolysis setup of the electrooxidation of RB in a continuous-flow electrolyzer.

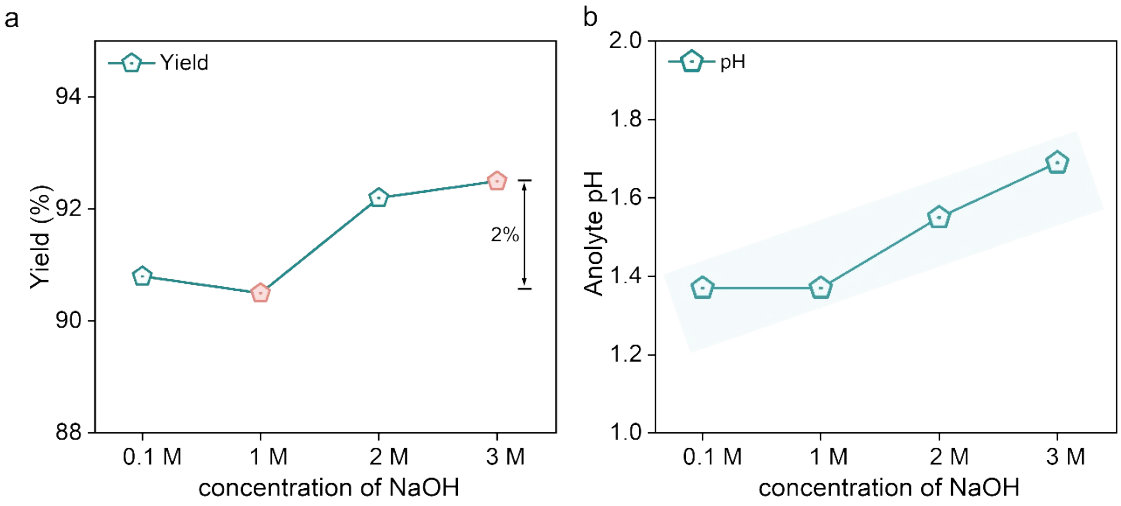

Fig. S18 (a) RO yield in different concentration of NaOH. (b) Electrolyte pH of the anode side after reaction.

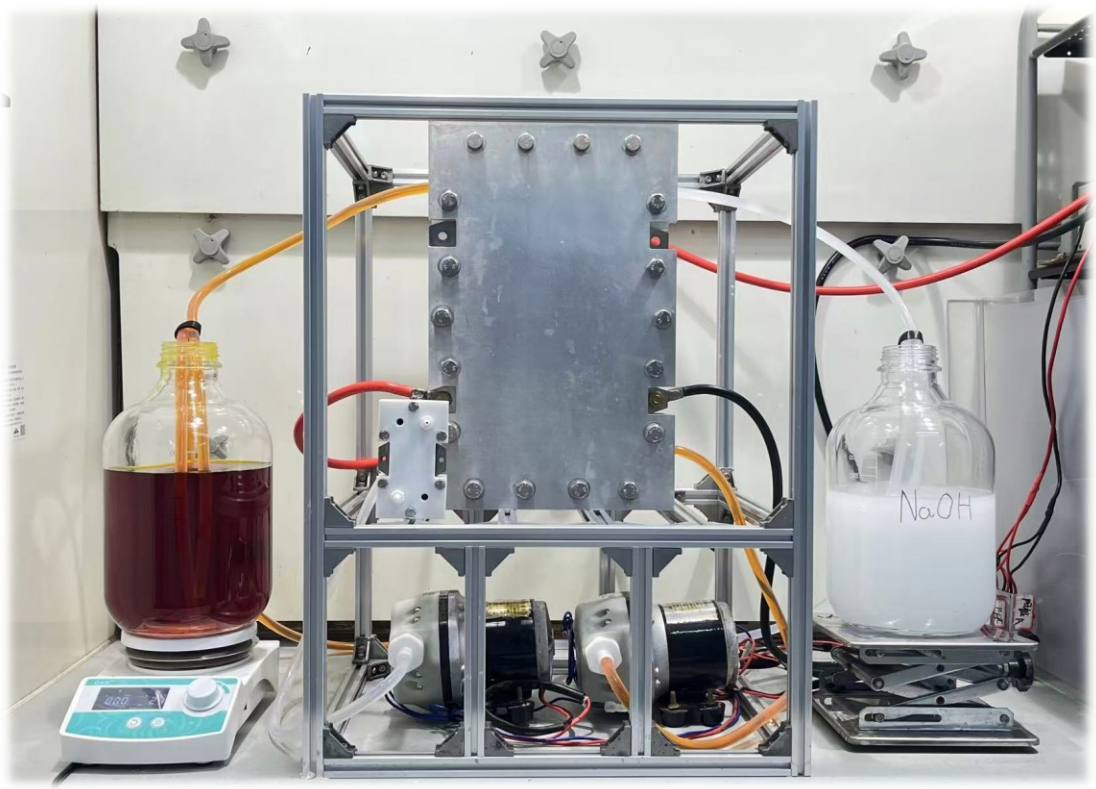

Fig. S19 Electrooxidation of RB on 50g scale

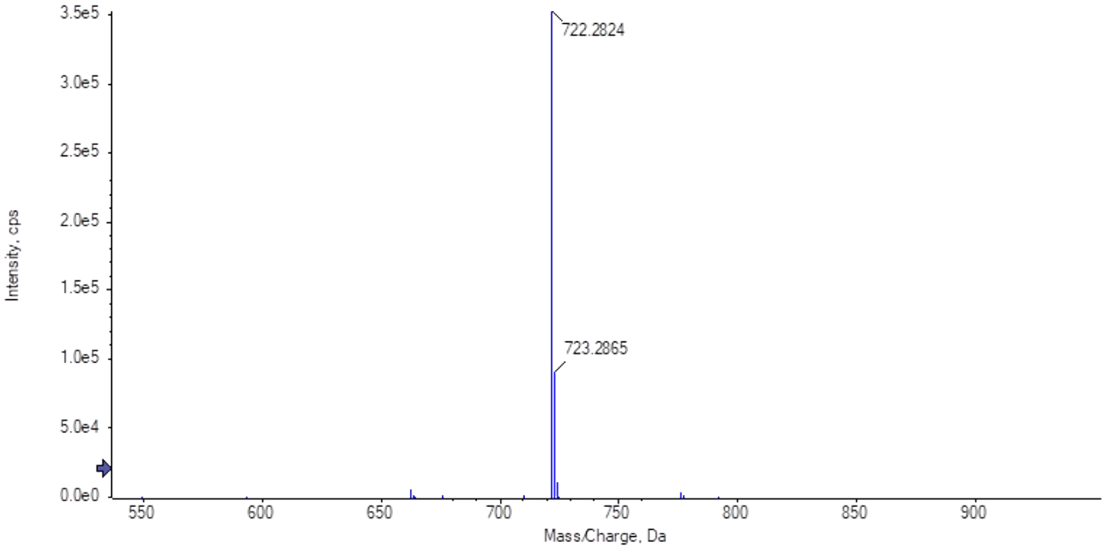

Ion Formula	Calculated *m/z*	Error (ppm)	Error (mmu)	RDB
C38H44NO13	722.28072	2.4	1.71	18.0

Fig. S20 Mass spectrum of RO.

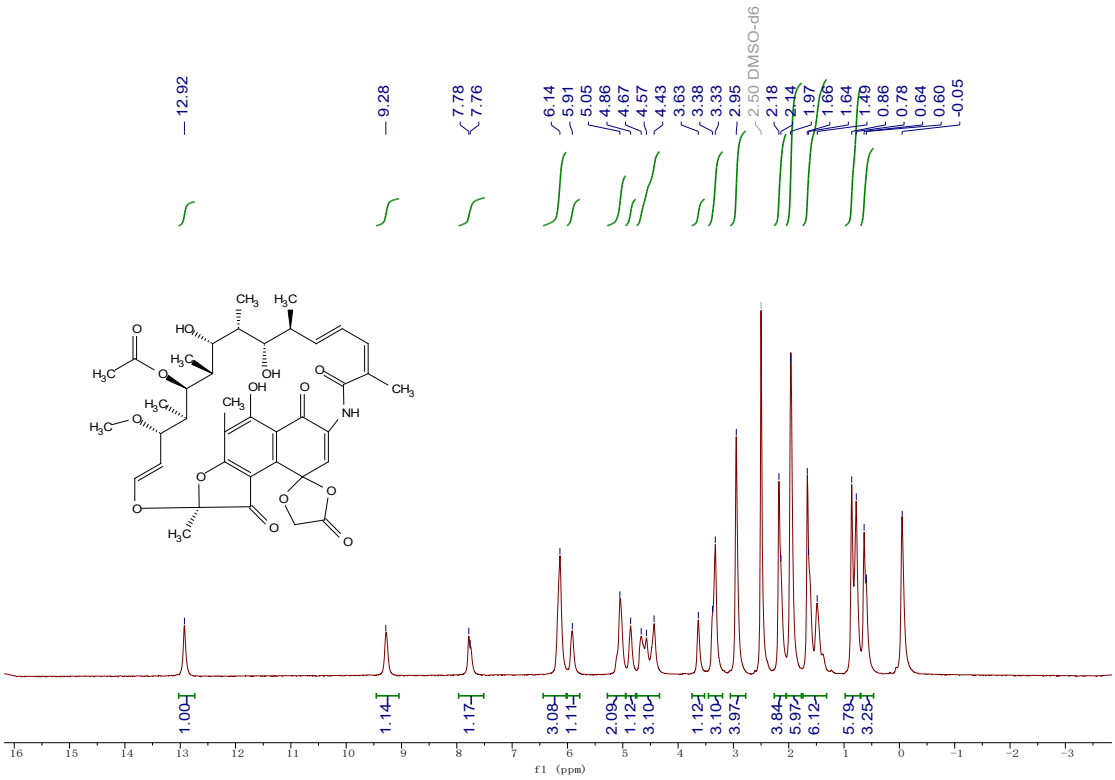

Fig. S21 ^{1}H NMR spectra of RO.

^{1}H NMR (600 MHz, DMSO-d6) δ 12.92 (s, 1H), 9.28 (s, 1H), 7.78 (s, 1H), 6.14 (s, 3H), 5.91 (s, 1H), 5.05 (s, 2H), 4.86 (s, 1H), 4.55 (d, J = 139.5 Hz, 3H), 3.63 (s, 1H), 3.35 (d, J = 30.0 Hz, 3H), 2.95 (s, 4H), 2.16 (d, J = 21.1 Hz, 4H), 1.97 (s, 6H), 1.58 (d, J = 107.5 Hz, 6H), 0.82 (d, J = 49.8 Hz, 6H), 0.62 (d, J = 24.9 Hz, 3H).

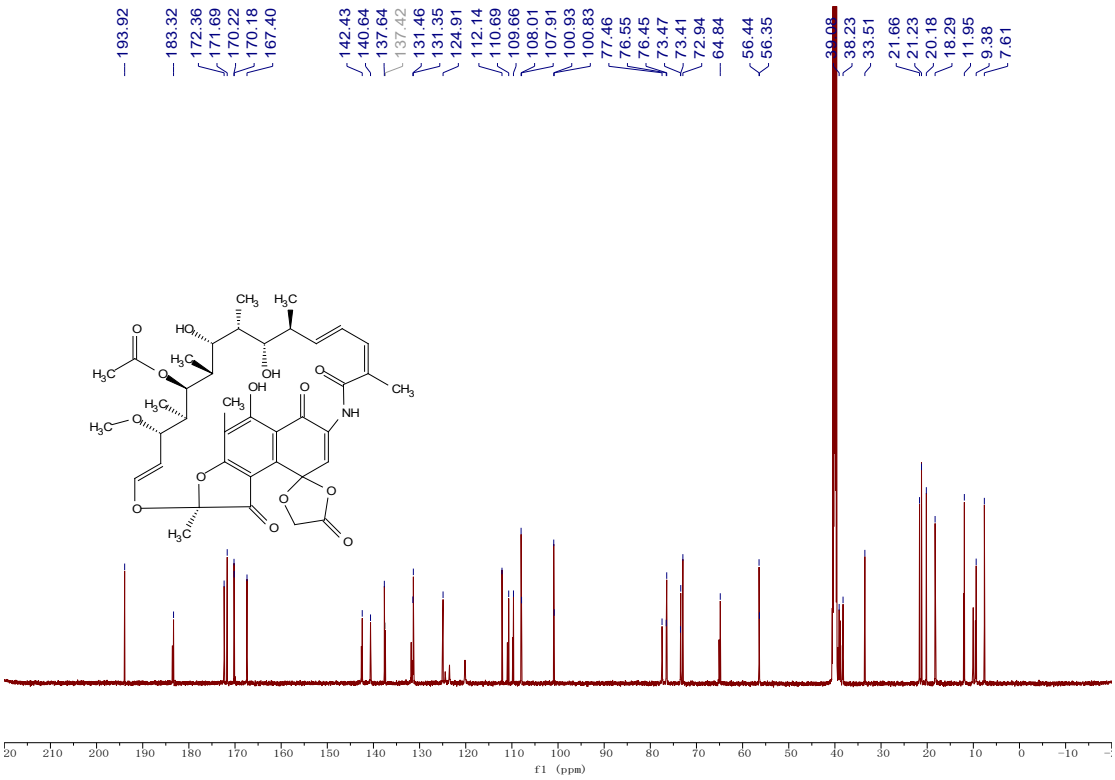

Fig. S22 ^{13}C NMR spectra of RO.

^{13}C NMR (151 MHz, DMSO-d6) δ 193.92, 183.32, 172.36, 171.69, 170.22, 170.18, 167.40, 142.43, 140.64, 137.64, 131.46, 131.35, 124.91, 112.14, 110.69, 109.66, 108.01, 107.91, 100.93, 100.83, 77.46, 76.55, 76.45, 73.47, 73.41, 72.94, 64.84, 56.44, 56.35, 39.08, 38.23, 33.51, 21.66, 21.23, 20.18, 18.29, 11.95, 9.38, 7.61.